A Wind Power Forecasting System to Optimize Grid Integration

William P. Mahoney, Keith Parks, Gerry Wiener, Yubao Liu, William L. Myers, Juanzhen Sun,
Luca Delle Monache, Thomas Hopson, David Johnson, and Sue Ellen Haupt

Abstract—Wind power forecasting can enhance the value of wind energy by improving the reliability of integrating this variable resource and improving the economic feasibility. The National Center for Atmospheric Research (NCAR) has collaborated with Xcel Energy to develop a multifaceted wind power prediction system. Both the day-ahead forecast that is used in trading and the short-term forecast are critical to economic decision making.

This wind power forecasting system includes high resolution and ensemble modeling capabilities, data assimilation, nowcasting, and statistical postprocessing technologies. The system utilizes publicly available model data and observations as well as wind forecasts produced from an NCAR-developed deterministic mesoscale wind forecast model with real-time four-dimensional data assimilation and a 30-member model ensemble system, which is calibrated using an Analogue Ensemble Kalman Filter and Quantile Regression. The model forecast data are combined using NCAR's Dynamic Integrated Forecast System (DICast). This system has substantially improved Xcel's overall ability to incorporate wind energy into their power mix.

Index Terms—Data assimilation, forecasting, nowcasting, wind energy, wind power forecasting.

I. INTRODUCTION

A. Motivation

THE recent policy trend to move the U.S. toward a larger fraction of the energy portfolio devoted to renewable energy sources [1] puts additional strain on the energy industry as these sources have to date been less predictable than traditional generation sources. Improved weather prediction and precise spatial analysis of mesoscale weather events are crucial to both short- and long-term energy management. There is a need to further develop and implement advanced weather observation and prediction technologies for the energy industry that benefit both public and private sectors [2]. Weather data and information are crucial to infrastructure planning and management, prediction of energy demand, management of energy supply, en-
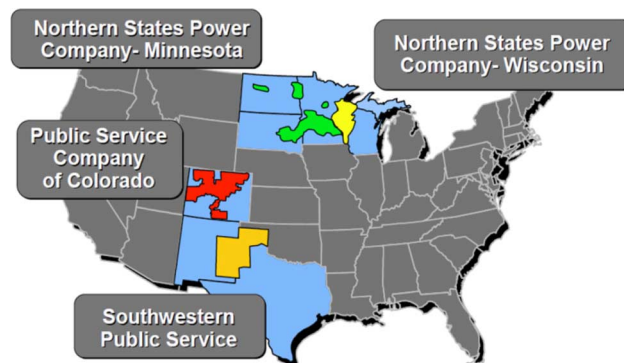
Fig. 1. Xcel Energy service areas.

ergy pricing and markets, energy system operations and regulatory compliance, and economic risk minimization [3].

B. Background

With 3.4 million electric customers, Xcel Energy is the fifth largest combined electric and gas utility in the United States. It is comprised of three separate service regions: Northern States Power (NSP), Public Service Company of Colorado (PSCo), and Southwestern Public Service (SPS). These regions are mapped in Fig. 1.

Xcel Energy boasts the largest wind energy capacity in the U.S. with more than 50 wind farms, 2972 turbines, and 4062-MW power. With wind capacity rising rapidly, Xcel Energy realized that improvements in wind energy prediction skill are required to reduce the cost of wind integration because this variable resource must be efficiently integrated into the grid to both minimize costs of day-ahead trading and to provide reliable and economic dispatch on a real-time basis. Thus, to meet Xcel Energy's growing need for wind energy prediction improvements, they forged a collaborative research and development effort in late 2008 to configure and build a comprehensive wind power forecasting system. An initial capability was rolled out in June 2009 and the more complete system was online in October 2009. After the system was implemented by Xcel Energy in 2011, the capabilities have been refined and updated by NCAR. This paper provides an overview of the entire system with some details on each of the components. For more detail on each of the system components, the reader is referred to the references.

C. System Overview

Our philosophy is to blend forecasting technologies and statistical methods that each provide useful information at
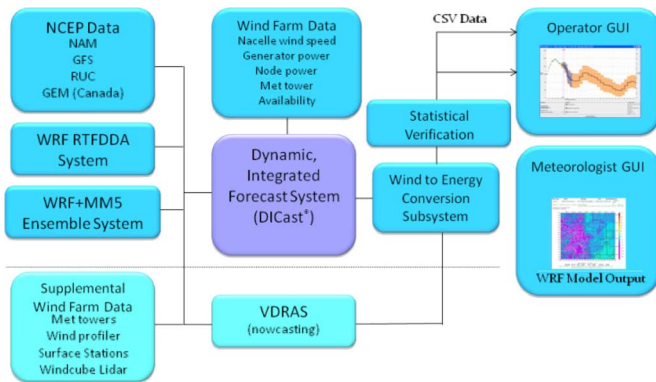
Fig. 2. Flowchart of the NCAR/Xcel Energy wind power forecasting system components.

some specific forecast lead-times covering Xcel Energy's 168 h forecast period so that the system as a whole merges all of those inputs to produce an optimized forecast at each lead time. Fig. 2 provides a flowchart of the NCAR/Xcel Energy wind power forecasting system components. Input data include weather model data from the National Centers for Environmental Prediction (NCEP) including the Global Forecast System (GFS), North American Mesoscale (NAM) Model, and Rapid Update Cycle (RUC) Model, and the Canadian Meteorological Centre's Global Environmental Multiscale (GEM) Model. NCEP Model Output Statistics (MOS) products are also utilized. In addition to ingesting forecast and MOS data from the operational centers, data from NCAR's own modeling systems are utilized. NCAR configured and tailored a version of the Weather Research and Forecasting (WRF) model and also configured a 30-member model ensemble system that uses both WRF and the Penn State-NCAR MM5 model (see Section II).

Wind turbine data are securely transmitted to the forecast system using an Xcel Energy PI interface node. At the center of the diagram lies the Dynamic Integrated ForeCast System (DICast). Its purpose is to bias correct all model input and to provide the best weights for those model data from its statistical learning methods (see Section III). DICast is trained to match the forecasts to the nacelle anemometer wind speeds at each turbine. This approach allows the system to take into account availability information that Xcel requires from the individual wind farms.

The consensus wind forecast for each turbine is then converted to power using various statistical approaches. The wind energy forecast data for each turbine and connection node are provided to Xcel Energy directly using comma delimited files, and via tailored Graphical User Interfaces (GUIs). The operators are provided with a GUI of projected power output plus historically derived error bars denoting the 25% and 75% uncertainty levels. In addition, a GUI showing the deterministic and ensemble model system output is provided to Xcel Energy meteorologists. These include standard weather maps available for each domain at different heights; wind, temperature, and humidity profiles at each wind farm; and wind power density maps at 50, 80, and 120 m above ground level. For the probabilistic forecasting, the ensemble mean, spread, meteograms, wind roses, likelihood of ramp event magnitudes and timing,

and exceedance probabilities for wind threshold plots are provided.

Below the dashed line in Fig. 2 is depicted the experimental wind nowcasting systems. The Variational Doppler Radar Assimilation System (VDRAS) uses four-dimensional variational (4 DVar) assimilation techniques to blend Doppler radar data into a cloud-scale model to provide a physically balanced current state of the atmosphere (Section IV).

The remainder of the paper provides details of the system components. Section V discusses the economic benefits of this system and the summary and conclusions appear in Section VI.

II. MODELING COMPONENT

A. Overview

Wind power management requires accurate current and look-ahead regional and local-scale (tens to hundreds kilometers) weather information. To analyze and predict wind flows near nacelle height, the weather prediction model is designed to resolve important details of forcing from complex terrain, land-water contrasts, and the heterogeneities of land surface properties that affect the wind characteristics. Furthermore, the modeling system is designed to avoid the "spin-up" problem that is manifested as spurious oscillations in the first few hours due to the inconsistencies between the analyzed initial conditions and the model's mathematical equations. To help alleviate these issues, NCAR implements a multiscale, rapid-cycling modeling system that includes assimilation techniques to initialize both the WRF [4] and Penn State-NCAR MM5 models [5].

The WRF model is a next-generation numerical weather prediction model developed by multiple U.S. government agencies and a large international research community. NCAR tests and distributes the code to the weather research and operational communities. WRF features multiple dynamical cores, a growing suite of data assimilation systems, and a software architecture that allows for computational parallelism and system extensibility. WRF is suitable for a broad spectrum of applications across scales ranging from tens of meters to thousands of kilometers.

A key feature of the modeling system is assimilating observations into the model background to produce an analysis, which provides a "best guess" initial condition for the model integration. This Real-Time Four-Dimension Data Assimilation (RTFDDA) system is based on Newtonian Relaxation, commonly known as nudging [6]–[8]. The NCAR RTFDDA system was originally developed for supporting operations at the Army test ranges [9], [10] as well as many other weather-critical applications [11]. The RTFDDA continuous data assimilation scheme utilizes all weather observations within an application domain. The continuous data assimilation applied during the analysis stage is able to provide "spun-up" initial conditions for each forecast cycle, thus producing four-dimensional dynamically balanced and physically consistent analyses and forecasts.

B. Deterministic Model System Configuration

The deterministic WRF modeling system was configured to cover Xcel Energy's service regions, with three nested grids at
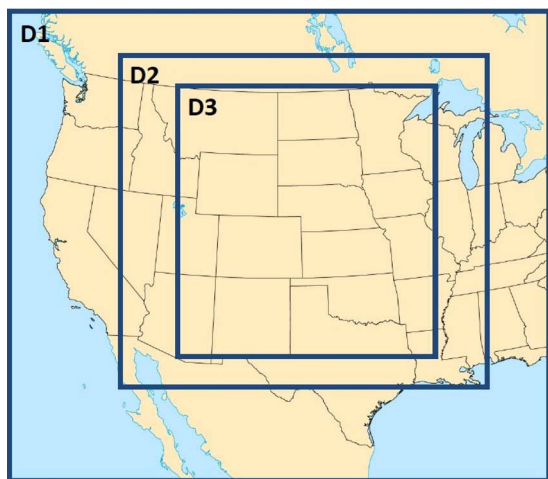
Fig. 3. Domain maps of the three-domain Xcel Energy deterministic WRF-RTFDDA forecasting system (D1, D2, and D3) and the two-domain 30-member ensemble probabilistic forecasting system (D1 and D3)).

30-, 10-, and 3.3-km grid spacing (Fig. 3). The RTFDDA system assimilates diverse observations including World Meteorological Organization (WMO) Global Telecommunication System (GTS) standard upper-air and surface stations, National Oceanic and Atmospheric Administration (NOAA) wind profilers, co-operative agency wind profilers, aircraft weather reports, satellite derived atmospheric winds, Doppler radar wind profiles, a large number of surface mesonet and other weather data sources, as well as wind farm meteorological tower and turbine nacelle anemometer wind speed measurements. This system is run eight times a day, and in each cycle, produces 24-h forecasts on the fine mesh (3.3 km) domain, output every 15 min, as well as producing a 72-h forecast for the two coarser domains, output hourly [12].

C. Probabilistic Prediction With an Ensemble System

Atmospheric processes are chaotic, implying inherent uncertainty, and weather models inevitably contain errors and uncertainties in various model components, including imperfect specification of model initial conditions and lateral boundary conditions, truncation errors, and physical process approximations (cloud physics, radiation, eddy diffusion, land surface, etc.). Therefore, it is appropriate to use weather prediction technologies that are designed to approximate forecast errors and uncertainties.

In addition to the deterministic RTFDDA component, NCAR implemented the mesoscale Ensemble Real-Time Four-Dimensional Data Assimilation (E-RTFDDA) system based on the probabilistic forecasting technology originally developed for Army test ranges [13]. The E-RTFDDA contains diverse ensemble perturbation approaches that consider uncertainties in all major system components. The system includes multiscale continuous-cycling probabilistic data assimilation and forecasting. The Xcel Energy E-RTFDDA system has 30 members, with 15 members based on the PSU-NCAR MM5 model and the other 15 members based on WRF. Because the ensemble model simulations are computationally costly, the ensemble model runs on two nested-grid domains with 30- and 10-km

grids. The 30-km grid is the same as the domain (D1 in Fig. 3) of the deterministic WRF RTFDDA model, but the 10-km grid is only run on the D3 domain. Furthermore, the ensemble system runs four forecast cycles a day, producing 6-h analyses and 48-h forecasts in each cycle.

D. Bias Correction and Ensemble Calibration

Since errors in physical model forecasts are inevitable, statistically postprocessing the model wind forecasts is beneficial. Two statistical postprocessing approaches are employed in the wind power modeling system. The first technique is the ANalog-space Kalman Filter (ANKF) that corrects the bias errors of the WRF RTFDDA forecasts; and the second is a quantile regression (QR) calibration scheme. Both ANKF and QR require a significant recent history of the model forecast data and wind plant measurements.

The theory behind both schemes is that the model's past performance, particularly the model error information for the weather scenarios that are similar to the current forecasts, is highly valuable for correcting the error of the current prediction.

ANKF was built upon the Kalman Filter (KF)-based bias correction technique [14], [15]. It was applied as a postprocessing component for the Xcel Energy single high-resolution deterministic forecast system [16]. The KF approach continuously adjusts/updates the prediction of bias using a Kalman gain, which weights more recent forecasts higher. In contrast, the new ANKF approach is formulated to rearrange the training data set from the worst to the best analog, and to apply the largest weights to the analogs that better match the current prediction.

QR ensemble calibration technologies [17] tune the reliability of the probabilistic prediction. The QR approach corrects the mean and all quantiles of the wind forecast bias as well as improving ensemble resolution and, more indirectly, exceedance probability forecasts (e.g., probability of wind speed > 10 m/s). The ANKF and QR techniques have been applied to the Xcel Energy ensemble forecasting system. With the combined ANKF-QR scheme, ANKF is performed independently for each of the 30 members of E-RTFDDA, and then these bias-corrected forecasts are fed into the QR module to generate calibrated probabilistic wind predictions.

E. Performance Assessment

To demonstrate the performance of the modeling system component for the wind-farm averaged 80-m wind speed, the skill score of ANKF, QR, and ANKF+QR with respect to the raw Xcel Energy ensemble-mean RFTDDA forecast is shown in Fig. 4 for a representative wind farm during December 2010. Similar results were obtained at other locations and for different periods (not shown). Note that the skill score is positively oriented with larger values indicating improvements over the raw ensemble mean as measured by a reduction in the RMSE. After the ANKF correction is applied to every ensemble member, the resulting improvement of the ensemble mean is in the 10%–20% range across the different forecast lead times. QR, which is applied to the entire ensemble distribution, shows similar skill, with a remarkable improvement for the first two forecast lead times in the range of 20%–50%. The higher range of improvements result from the QR, which includes
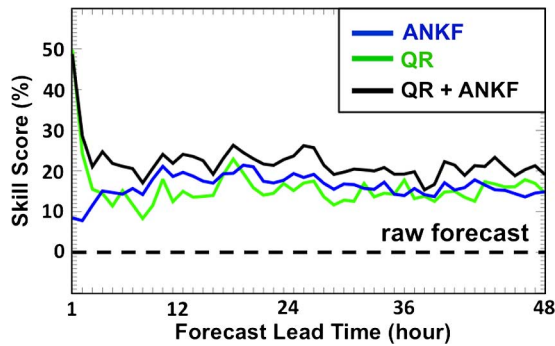
Fig. 4. Skill score (%) versus forecast lead time (hour) of ANKF, QR, and ANKF+QR with respect to the raw Xcel Energy ensemble-mean RFTDDA forecast [as measured by root-mean-square error (RMSE)], for 80-m wind speed averaged over all turbines of a wind farm during December 2010. Positive values correspond to percentage improvement (i.e., lower RMSE) with respect the raw forecast.

persistence as one of the predictors to optimize the correction. Interestingly, given the different design and correction strategy of the methods—ANKF is applied to each individual ensemble member whereas QR is a calibration procedure that corrects the entire ensemble distribution—applying both methods (ANKF+QR) results in the best correction. Indeed, ANKF+QR preserves the large improvements (20%–50%) in the first two hours and produces a better correction than either ANKF or QR alone, with improvements in the 15%–25% range for forecast lead times from 3 to 48 hour.

III. STATISTICAL POSTPROCESSING

A. Dynamic Integrated ForeCast System

A centerpiece of the forecast system is DICast, which tunes, integrates, and optimizes the contributions of the individual component forecasts. DICast is a robust consensus forecast system. Its role is to integrate a variety of data and produce a single, optimized forecast for each user defined site [18].

The main inputs are weather forecast datasets and weather observations. In this application, DICast generates an optimized consensus hub height wind speed forecast for each wind turbine. Downstream processes are responsible for turning these wind speed forecasts into turbine-specific power forecasts and aggregating these into farm and connection node power forecasts. DICast generates new wind speed forecasts every hour by taking advantage of the latest available forecast (e.g., model, MOS) and observational data. A forward error correction scheme is then applied every 15 min for the first 3 h of the forecast period.

1) DICast Input Data: The Xcel Energy version of DICast currently uses seven input models. The publicly available models include NCEP's GFS, NAM, and RUC as well as the Canadian GEM model. In addition, it ingests the high-resolution (3.3-km grid) deterministic WRF RTFDDA simulation and the means from each of the two 15-member WRF and MM5 model ensembles (10-km grid). For each input model, only the most recent model run is used. This means that, for example, once the 12Z GFS run has arrived, the previous 06Z GFS run is no longer used in the real-time forecasting process.

2) Observational Input Data: Observational data are critical to DICast. As an automated learning system, it depends on an historical observational dataset to serve as "ground truth." The ultimate goal in this application is to predict power generation by a turbine. The environmental measurement most closely related to turbine power is wind speed. Thus, DICast focuses on predicting wind speed at hub height.

The two choices of wind speed observations are the anemometer installed at the meteorological tower at the farm, and/or the nacelle anemometers mounted atop each turbine generator. The meteorological tower anemometer, where available, provides a better measurement of the free atmospheric wind than the nacelle anemometers because the latter are positioned behind the rotating turbine blades that disturb the flow. However, studies have shown that while DICast can generate tuned forecasts at the meteorological towers, neither the resultant forecasts nor the statistical equations work well at the individual turbines. Thus we instead focus on the nacelle wind speed measurements. Although these data do not accurately represent the free atmospheric flow, they have a strong correlation to turbine power based on a large empirical database.

The raw nacelle observations are available at high frequency, exceeding one per minute. Due to the gusty nature of wind, these observations are often noisy. Here we use 15-min averages of the measured wind speed, which are more statistically representative of the wind and power produced during that period.

3) Dynamic Model Output Statistics (DMOS): Dynamic Model Output Statistics (DMOS) is the first forecast optimization step in the DICast forecast process. The goal is to optimize the forecast from each model independently based on available observation verification data. DMOS finds relationships between each model's data and the observations valid at a particular time of day. DMOS accomplishes this through an objective statistical process similar to the National Weather Service's (NWS) Model Output Statistics (MOS) process [19]. Unfortunately, the NWS does not provide optimized MOS products at locations or heights relevant to wind energy forecasting. Thus, we train to the nacelle anemometer data to generate an optimized forecast of each anemometer based on the input models.

The main difficulty with using NWP model data in the prediction of hub height wind speed is that models do not directly predict the wind speed at hub height. Two main classes of model output exist. In the first, data above the surface is provided on specific pressure levels. Model data from NCEP, the Canadian Meteorological Center (CMC) and the European Center for Medium Range Forecasting (ECMWF) are provided in this format. The spacing between these pressure levels varies but is usually 25 millibars or more near the surface. This translates to roughly 250 m between relevant data points in the vertical. In these models, that will often mean that the first pressure level may actually be below the model's earth surface. This is an interesting complexity since some of the models, e.g. NAM, forecast only above the surface and yet their output is modified to match earlier versions of the model's output grid. The coarse vertical resolution is mitigated somewhat by the existence of a 10-m above ground level (AGL) wind forecast variable in these

models. This model variable adds significant value to the DMOS forecast optimization process. In this class of models, very significant reductions in forecast error are possible.

The second class of models use a terrain following coordinate system. The output of these models is provided at sigma levels, i.e., specific levels above the ground. They are configured to have several closely spaced levels near the surface, e.g., 60 and 100 m. The number and density of levels is determined by trading off vertical resolution with compute speed. Models with output in this format require less interpolation in the vertical. Since this output is more specific to the height of the hub, the forecast error reductions realized by applying DICast are less than for the first class of models.

New DMOS regression equations are generated every week. The DMOS system configured for Xcel Energy uses the last 90 days for forecast predictors and observation pairs when determining the best statistical relationship. Our analysis has shown that less than 90 days provides less stable regression equations, while longer training periods provide marginal benefits and may introduce seasonal effects.

Sometimes during the DMOS calculation process, a satisfactory regression equation cannot be generated from the predictor/observational history due to insufficient history or to not finding a regression equation with sufficiently high correlation. In this case, a forecast can still be made by using one of the predictors derived from the model. The predictor used in this case is called the default predictor and is chosen by examining which of the predictors has performed well historically in that turbine's region. The use of a default predictor provides robustness to the system and allows it to always produce a forecast for each turbine in the system. The most common cases where the default predictor is used are: 1) initial forecasts before sufficient history has been accumulated; 2) an anemometer's data does not get into the system due to telecommunication issues; and 3) the anemometer suffers from quality control issues and has a number of bad data points that survive quality control procedures.

As new model data are ingested, the hub height wind speed predictors are extracted and stored. To complete the process of making a DMOS forecast, the previously calculated regression equation specific to this model run time, site, and lead time is used with these new predictors. This linear combination of the current predictors produces the forecast value. While calculation of the regression equation may be computationally expensive, this application of that equation to the current equation is very fast.

Fig. 5 plots the forecast root mean squared error (RMSE) of individual predictors from the 12Z NAM run for the 1976 Xcel Energy turbines operating during the month of January 2010. The diurnal cycle is obvious in the errors as well as the expected general increasing trend in error with lead time. Each line on Fig. 5 represents the forecast error of one of the NAM hub height wind speed predictors. Some predictors' forecasts are much more accurate during the day yet are less accurate at night. Others have fairly consistent error characteristics throughout the diurnal cycle and across the entire forecast period. The NAM 10-m wind speed (predictor number 2304) was particularly poor for direct use as the hub height wind speed
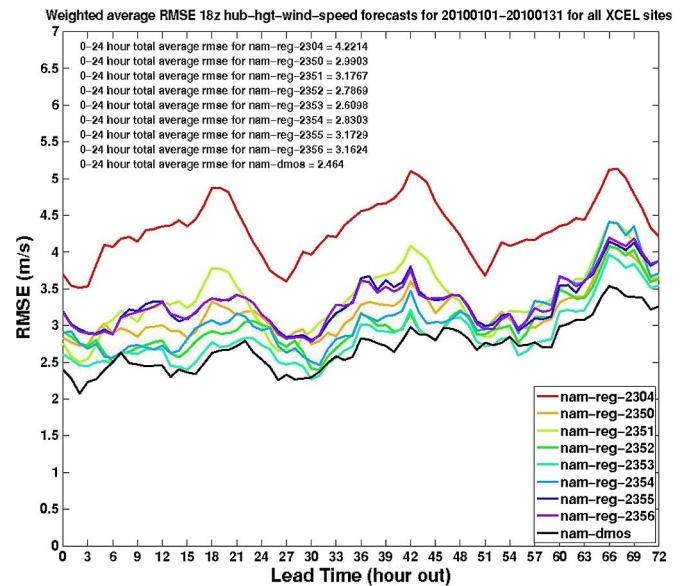

Fig. 5. Root-mean-squared errors for individual wind speed predictors compared to the NAM DMOS forecast made in January 2010 for 1976 turbines. The NAM DMOS forecast generated by DICast is the black line with consistently lowest RMSE.

forecast during this month. This observation highlights the difference in wind speeds at hub height (80–100 m) compared to the traditionally forecast near-surface wind speeds.

While these 1976 sites represent a statistically significant sample, it is important to remember that although a predictor may perform poorly overall, it may be excellent at certain sites, and thus can be of value to the forecast at these sites. Each predictor has its strengths and weaknesses. No predictor should be removed from the process unless it does not significantly contribute at any site and at any time. In fact, although the 10 m wind speed is a poor standalone predictor, it is less correlated with the pressure-level winds, and thus often is used in combination with the other predictors during the DMOS process. The error for the DICast DMOS forecast is plotted as the black line below the other error lines in Fig. 5. Thus, it is statistically better than any of the individual predictors at all lead times out to 72 h.

Each month, the relative skills of the predictors change. That is, the best predictor one month may not be best in the following month. In spite of the constant change in skill in the predictors, the DMOS forecast is, by construction, always statistically better than the individual "predictor of the month." Thus DMOS provides both a level of optimization and robustness to the forecast process.

4) Forecast Integration: Once the DMOS process has generated optimized forecasts from individual forecast models, DICast combines these forecasts to produce a consensus forecast. At each forecast location and lead time, comparison of the observations and the individual models' DMOS forecasts are used to determine which models have performed better than others in the recent past and gives more weight to the better performers.

Since the model's data arrive asynchronously, the best model may vary from hour to hour. That is, a "fresh" model is often better than older models. Assuming that the model data output

times are predictable, development of weights specific to each model's skill at a specific forecast generation time is merited. For the Xcel Energy system, in which DICast forecasts are generated hourly, there are 24 complete sets of weights—one for each forecast generation hour of the day—each with weights specific to each site and forecast lead time. In each complete set of weights, there are weight vectors specific to each wind turbine site and lead time.

DICast creates its consensus as a bias-corrected weighted sum of input forecasts

$$F = (\Sigma w_i f_i)/(\Sigma w_i) + \text{Bias} \qquad (1)$$

where f_i are the forecast values and w_i are the weights. Missing forecasts are removed from the consensus. This is a computationally simple, yet effective, forecast combination method. More complex combination schemes are possible, but in our experience, the marginal improvement does not merit the additional complexity.

Each day the integrator examines how well it performed on the previous day's forecast and uses that information to nudge its weights toward an improved consensus. Because of the models' spatial and temporal performance differences, the integrator's combination will differ for each site, lead time, and forecast generation time.

By design, the DICast system is robust in its ability to produce quality forecasts despite the unavailability of one or more of the input forecast models. When one model's data has not arrived at its expected arrival time, the last available run is used until new data arrives. This may lead to a small degradation in forecast quality that is rectified at the next model run cycle.

A variety of weight calculation approaches are possible. These are compared and summarized in several papers [20]–[22]. The adaptive learning approach taken in the DICast integrator was chosen for several reasons. First, it is computationally simple and robust. Second, it can easily adapt to the addition of new input forecast models or the removal of obsolete models. Finally, new sites can be added to the system and, with an initial default weight set, forecasts can be made almost immediately. These weights will rapidly evolve toward a nearly optimal solution [23].

Each day, the weights are modified in the direction of the gradient in weight space. That is, the vector of weights is nudged in the direction of steepest descent of the error (the difference between the verification v_i and the forecast values)

$$\Delta w_i = S^* \left(\frac{\partial}{\partial w_i} \right) \left\{ (v_i - f_i)^2 \right\}. \qquad (2)$$

The step length S is a parameter determined by the user to affect how quickly the system adapts. The choice of S effectively trades off the initial discovery of the optimal combination against the daily update magnitude. Unless the step size is too large, the updated weights would have, by design, led to a forecast with a smaller error had they been used for the previous day's forecast. There is also a cap on the magnitude of any change so that one day's missed forecast does not completely alter a set of weights that work reasonably well.
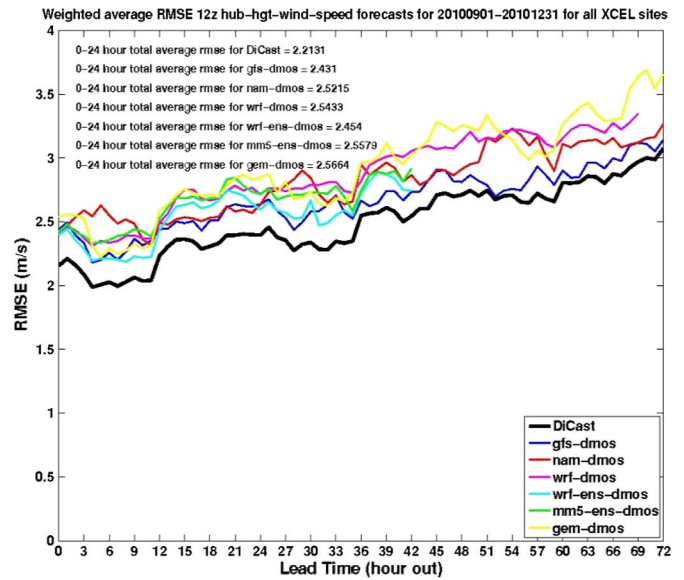

Fig. 6. Errors for DMOS forecasts compared to the DICast integrated forecast made for October, November, and December 2010. The DICast integrated forecast is the black line with consistently lowest RMSE.

In this way, the DICast integrator never attempts to directly calculate the optimal set of weights. Instead it takes an approach of pursuing the location of the minimum error. The location of the minimum is rarely stationary. It changes daily. In a larger sense, the nexus of the optimal vector changes seasonally to capture the variability in the models' skills. Other weight calculation approaches that examine a longer history require more computational resources. Due to the daily variability in model skill and observational representativeness, this additional computational cost is not merited.

The value of this consensus, multimodel approach and the implementation choices made within the DICast integrator are seen in Fig. 6. There, the errors of the individual DMOS optimized forecasts are compared to the errors of the DICast integrated forecast. The errors are shown for the first 72 forecast hours during the fall and early winter months of 2010. These statistics are for the same 1976 turbines used for Fig. 5.

The DICast integrated forecast made using these ingredients statistically outperforms every one of the ingredients by a substantial margin. During any given month, the integrated forecast typically outperforms the best "model of the month" with a reduction in forecast error of 10%–15%. Each month there is a reshuffling of the best models, yet the integrated forecast learns rapidly enough that it always has the best error characteristics. Studies of errors in wind power production indicate that this reduction in wind speed error directly translates into a comparable reduction in wind power generation error.

The results demonstrated in Fig. 6 argue strongly for a multimodel solution rather than using any single model solution in order to reduce the RMSE (or MAE) of the hub height wind speed forecast. This result is not unexpected: Eckel and Mass [24] have shown that when independent model data are added to a consensus forecast system, even if that model does not typically make a better forecast, its addition to the system improves the consensus forecast. The linkage between accuracy of wind
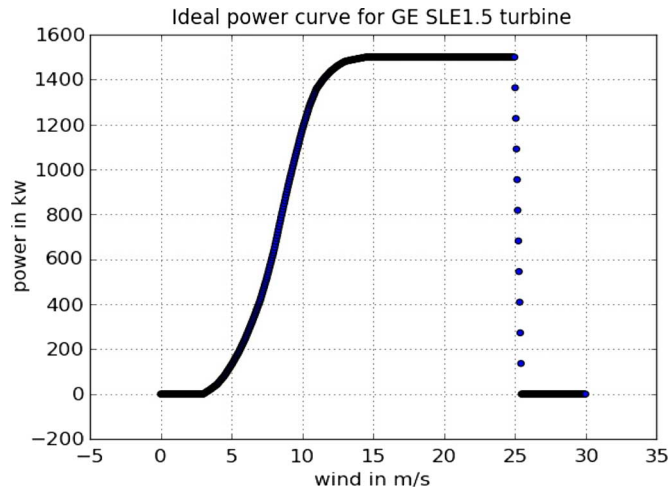
Fig. 7. Example manufacturer's power curve.

Fig. 9. Example scatter plot of empirical wind speed versus power relationship for a farm connection node.
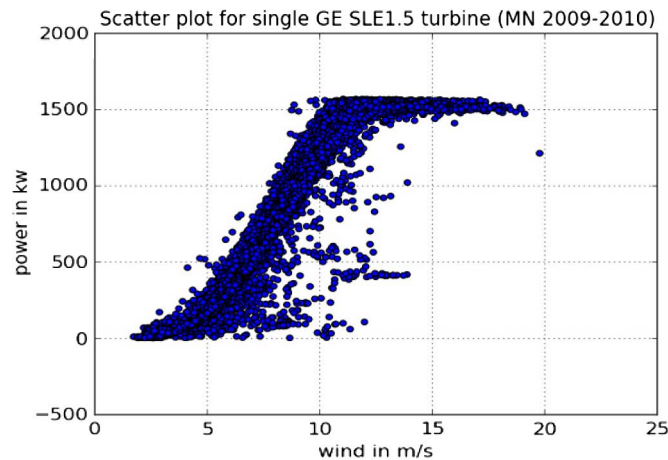

Fig. 8. Example scatter plot of empirical wind speed versus power relationship for a single turbine.

speed forecasts and power forecasts further establishes the benefits of consensus forecasting for hub height wind speeds. We note that DICast can be configured to produce similar reductions in error for other forecast variables, e.g., air temperature and dew point temperature.

B. Power Conversion

The next step in producing a wind power forecast is converting the DICast generated wind speed to power. It may seem natural to apply the turbine manufacturer's power curve to the wind speed forecast at each farm turbine and then to sum up the resulting powers. The manufacturer's power curve (see example in Fig. 7) as developed offers an idealized power output for each given turbine type as a function of wind speed assuming specific air density conditions and a minimal amount of turbulence and wind shear across the blade span.

Unfortunately, power production can often deviate substantially from the manufacturer's power curve (Fig. 8), which can lead to significant forecast power error. In examining Fig. 8, it is obvious that a single wind speed can correspond to a wide variety of power outputs; thus a simple one-to-one relationship is not achievable in practice.
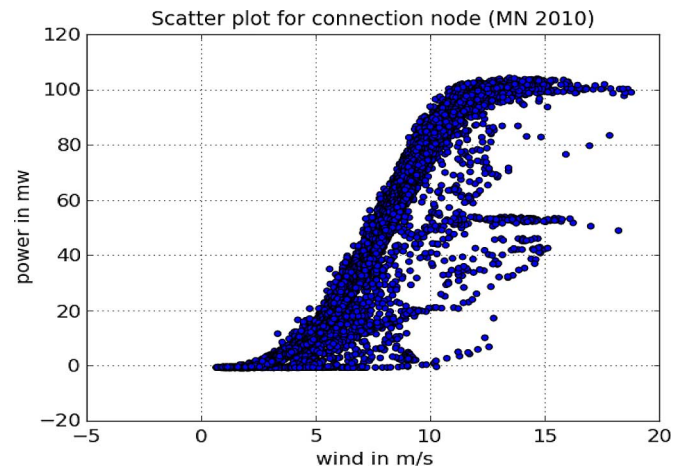
Power curves representing the total power at a farm connection node based on average observed nacelle wind speed tend to be better behaved owing to error cancellation, yet problems remain, as can be seen in Fig. 9.

One would expect that additional observations including wind direction, temperature and air pressure would assist in accounting for the above deviations from the ideal manufacturer's power curve, but such observations are generally not available owing to the general lack of maintained meteorological towers at current wind farms.

Since wind speed alone poorly accounts for turbine power, the Xcel Energy wind power system was designed to utilize historical wind and power. At farms where turbine observations are available, the mean nacelle wind speed and mean turbine power are calculated every 15 min. A training data set is formulated using: WindSpeed(t0), TurbinePower(t0), and WindSpeed(t1) as the predictors and TurbinePower(t1) as the predictand.

Here, WindSpeed(t0) is the nacelle wind speed at time t0, TurbinePower(t0) is the associated turbine power at time t0, WindSpeed(t1) is the nacelle wind speed at time t1 (15 min later) and TurbinePower(t1) is the desired associated turbine power at time t1. Different data mining techniques such as Random Forests, Regression Trees, K-Nearest Neighbor, etc. were tested to approximate TurbinePower(t1) using the previous three predictors and it was found that the regression tree Cubist[1] was one of the best performers and was easy to apply in practice.

In the actual implementation, the current nacelle wind speed, the current turbine power, and the next forecast nacelle wind speed are actually substituted into the data mining model in order to forecast the next turbine power value. Consecutive turbine power forecasts are then generated by utilizing consecutive wind forecasts and employing recursion. In case of missing observed nacelle winds and turbine power data, forecast wind speeds and ideal power curve estimated power are used in the above recursion. Finally, at farms where no wind/power observations are readily available, forecast wind speed is simply fed into the appropriate idealized power curve in order to determine generated power. It should be noted that Xcel Energy realized

---

[1]Cubist is a trademark of RuleQuest Research.

the benefit of having turbine data flow into their wind energy prediction system and hence implemented procedures to collect real-time data from their wind farms and to date, real-time data flow from approximately 80% of their installed capacity.

Once the turbine power is forecast for each turbine, the powers are summed for each connection node and operating region in order to estimate the overall connection node and regional power.

C. Power Forecast Error Calculation

The power forecasts are stored for a number of weeks to support ongoing forecast verification. The mean absolute error (MAE) is calculated for each connection node/forecast lead time pair. Forecast connection node power is compared to observed connection node power for each 15-min forecast out to 3-h and for each 60-min forecast out to 168-h. The MAE is normalized to a percentage error by dividing it by the connection node maximum capacity. All errors for a specific lead time are rolled-up over 7-day and 30-day periods in order to create short-term error statistics. No attempt is made currently to differentiate mean absolute percentage error based on different periods of the day such as day versus night, morning, afternoon, evening, etc.

D. Incorporating Forecast Availability Data

Wind turbines may be taken offline for routine or special maintenance and as a result the expected power production at affected farms may be substantially reduced. To account for this, the forecast system incorporates a percentage turbine availability forecast for each farm. The available power forecasts are produced by the contributing farms in accord with their maintenance schedules. This information is automatically incorporated in the production of an availability forecast that can be viewed separately from the full potential power forecast.

IV. NOWCASTING

Wind ramp events that correspond to mesoscale features, such as passages of cold fronts or thunderstorm outflows, pose a great challenge for wind power prediction. Such ramp events can cause rapid power increases or decreases over a short period of time [3], [25], [26]. Forecasting the timing, magnitude, and duration of these ramps can prove difficult. Although the basic wind forecasting system described above typically foresees significant power ramps, we wish to fine-tune the capability to accurately predict the timing, magnitude, and duration of an event, particularly those caused by mesoscale weather phenomena such as thunderstorm gust fronts. Accurately forecasting these events for wind power applications requires frequently refreshed wind field analyses with details at the scale that atmospheric convection can be resolved. Wind nowcasting based on such analyses with a forecast range up to a few hours are expected to provide improved wind information for wind energy prediction.

NCAR's Variational Doppler Radar Assimilation System (VDRAS) was designed to produce high-resolution and high-frequency atmospheric analyses using high-resolution observations from Doppler radars, lidars, and surface networks. VDRAS, which was originally developed to nowcast convective storms, has been developed and continually improved
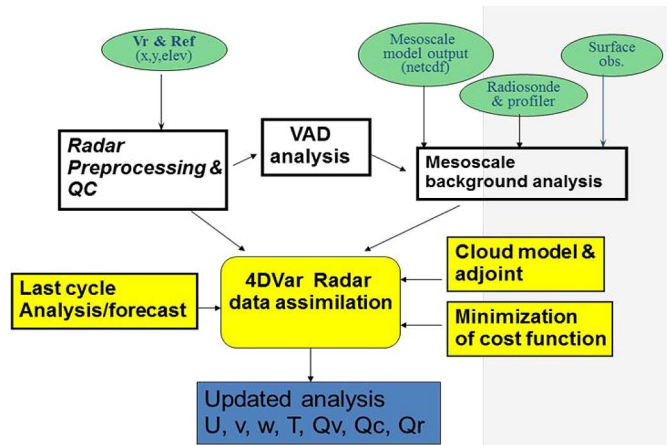

Fig. 10. VDRAS flowchart. The 4DVAR processes are shown in yellow.

by NCAR since the early 1990s. The system provides wind, thermodynamical, and microphysical analyses with a typical spatial resolution of 1–4 km and temporal update frequency of 15–20 min. VDRAS has been used extensively for research [27], [28] and has been installed for real-time nowcasting of convective weather domestically in a number of NWS offices [29], in U.S. Army test ranges, for homeland security applications, and internationally for the last two summer Olympics [30], [31]. Thus, it is logical to test this proven technology for wind ramp forecasting.

The major processes of VDRAS include data ingest, data preprocessing, data assimilation, and output generation (Fig. 10). The central process of VDRAS is the four-dimensional variational analysis (4DVAR) radar data assimilation, which includes a cloud-scale numerical model, the adjoint of the numerical model, a cost function, a minimization algorithm, background analysis, and the specification of background and observations error statistics. The numerical model used to represent the convective scale motion is anelastic with Kessler-type [30] warm rain microphysical parameterization and a simple ice scheme. There are six prognostic equations: one each for the three velocity components (u, v, and w), the liquid water potential temperature (θ_l), the total water mixing ratio (q_t), and the rainwater/snow mixing ratio (q_r/q_s). The pressure (p) is diagnosed through a Poisson equation. The temperature (T) and the cloud water/ice mixing ratio (q_c/q_i) are diagnosed from the prognostic variable by assuming that all vapor in excess of the saturation value is converted to cloud water (or ice depending on temperature).

The 4DVAR scheme in VDRAS fits the model prediction to observations over a specified time period; thereby a set of optimal initial conditions of the constraining numerical model that minimize a cost function can be obtained. The cost function includes three terms: a background term that measures the departure from a short forecast (typically 5 min) starting from the previous cycle 4DVAR analysis; an observation term that measures the difference between the radial velocity and reflectivity observations and their model counterparts; a mesoscale background term to ensure that the analysis is not too far from a mesoscale analysis. The detailed form of the cost function can be found in [33].

The mesoscale analysis is obtained using a 3-D objective analysis technique that combines conventional observations from radiosonde, profiler, Velocity Azimuth Display (VAD) profile from radar, and surface observations with a mesoscale model analysis as a first guess. These nonradar data and radar-derived VAD profiles are analyzed prior to the 4DVAR radar data assimilation to obtain a background environment for the convective-scale features that are represented by Doppler radars. This two-step approach enables the data assimilation system to take into account the different representative scales of the observations and allows the use of a small assimilation window (and hence a rapid update cycle) for the high-temporal resolution radar observations. The mesoscale analysis also provides boundary conditions for the subsequent radar data assimilation. The detailed description of the mesoscale analysis can be found in [33].

After the mesoscale background is obtained and the radar observations are preprocessed and quality-controlled, the VDRAS 4DVAR procedure (indicated by the yellow boxes in Fig. 10) is executed with the cloud model as the constraint with an assimilation window of 12 min. The cost function is minimized iteratively using a quasi-Newton conjugate gradient method with the gradient provided by the backward integration of the adjoint model. The forecast background represented in the first term of the cost function is obtained by integrating the cloud model 5 min forward after the 4DVAR assimilation is finished in the last cycle. With the temporal window of 12 min in the 4DVAR assimilation, 3 min in the 4DVAR assimilation, three scanning Doppler radar volumes are assimilated. The mesoscale analysis is updated at the start time of each 4DVAR assimilation cycle using updated surface observations and VAD analysis. The updated analyses of three-dimensional wind, temperature, water vapor, and microphysical variables are produced through the 4DVAR assimilation.

To test its applicability for observing wind ramps, VDRAS was installed over part of the Xcel Energy service area, covering wind farms in Colorado, New Mexico, and Texas (see Fig. 11) with an initial horizontal resolution of 4 km and a vertical resolution of 200 m. Low-level wind analyses are produced every 18 min by assimilating data from eight WSR-88D radars and METAR surface stations using WRF-RTFDDA as a background and first guess.

VDRAS wind analyses of several ramp cases have been analyzed and evaluated. Here, we report the results from two case studies (others are reported in [34]). The first case occurred on June 8, 2010 and featured a line of convective storms when a cold front passed through the wind farms in Northern Colorado near the border of Nebraska. A very strong cold pool developed as a cold front moved southeastward. The associated strong wind passed the wind farms in the Northern Colorado. The second ramp case occurred on July 10–11, 2010 and was associated with scattered convective activity in a dissipating stage.

Fig. 12 shows the VDRAS analyses of perturbation temperature [(a) and (b)] and wind speed [(c) and (d)]. Cold pools generated by dissipating convective cells are analyzed [(a) and (b)] and their evolutions from 230500 UTC to 000500 UTC are clearly shown by comparing (b) with (a). The cold pool in the northwest of the domain is the major cause of the wind ramp-up
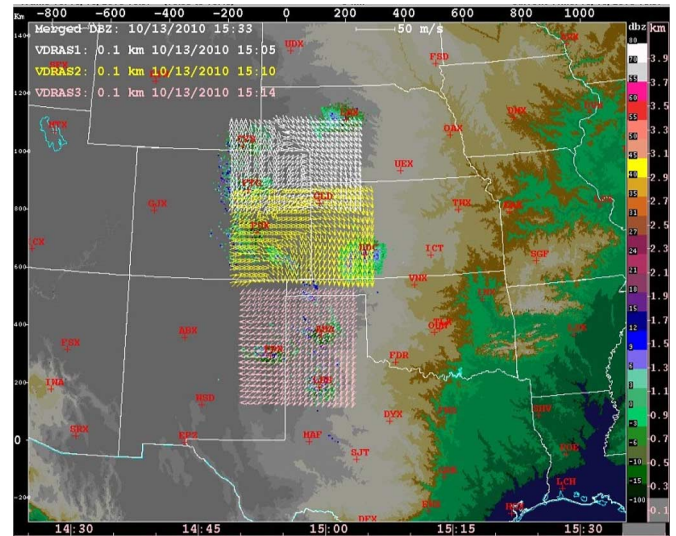

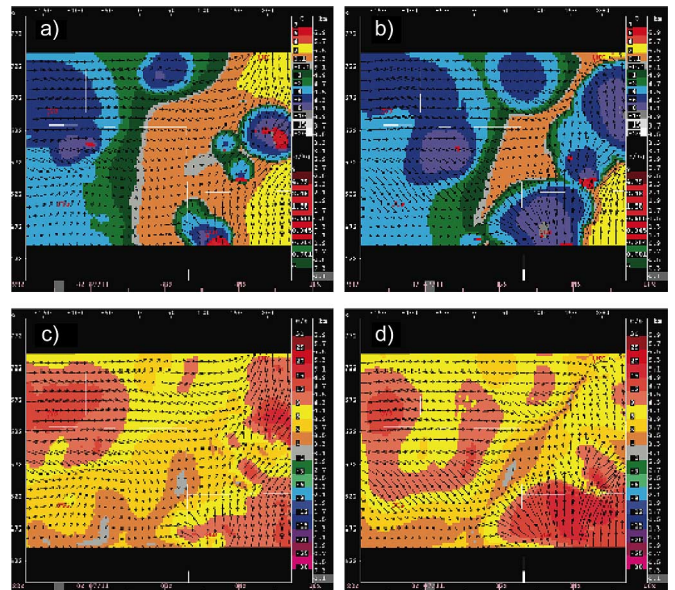Fig. 11.   VDRAS domains for Xcel Energy wind ramp nowcasting.

Fig. 12.   VDRAS analyses of perturbation temperature from the domain mean (a) at 230500 UTC, July 10 and (b) at 000500 UTC, July 11, and of wind speed (c) at 230500 UTC, July 10 and (d) at 000500 UTC, July 11. The horizontal wind vectors from VDRAS are overlaid in all panels. The reflectivity greater than 35 dBZ is shown in panels (a) and (b) by the red shade.

and wind ramp-down of the wind farms in Northern Colorado near the border of Colorado and Nebraska. The wind change is better shown by the wind speed plots in panels (c) and (d).

The VDRAS wind analyses at the lowest model level (100 m) are verified against observations at turbine hub height (approximately 70 m). Fig. 13 shows the verification results of the two study cases. The VDRAS wind agrees quite well with the turbine hub height wind for the July 10–11 case, while the ramp on June 8 from VDRAS has a 1-h delay. Preliminary examination shows that the delay is attributed to the high vertical shear of the wind on this day and the fact that the two types of data are not located at the same height (70 m for the turbine hub wind versus 100 m for VDRAS). An interpolation scheme is being developed to better approximate wind speed at turbine hub height.
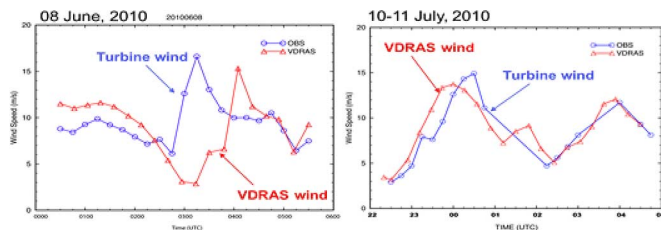
Fig. 13. Verification of VDRAS wind analyses against averaged turbine hub height wind observations at a Northern Colorado wind farm.

Fig. 14. Comparison of mean absolute error as a percentage of capacity between 2008 and 2011 for the PSCo service area.

Another solution to align the two winds is to run VDRAS with a higher vertical resolution so that the first model level coincides with the turbine hub height.

Obtaining accurate and updated analyses is only the first step toward improving 0- to 2-h nowcasting of ramp events. To estimate the future location of the features identified through VDRAS analyses, several approaches can be taken. One method is feature extrapolation, in which a feature (e.g., convergence line) that has been identified is advected with the wind, which can have either directional shifts or speed gradients within the domain. A second approach is to directly integrate the underlying VDRAS cloud-scale model. A previous study using VDRAS [35] suggests that the forecast of a gust front and its associated sudden wind change produces improved results when a 2-D advection velocity field was used instead of the 3-D velocity field from the VDRAS analysis. A third approach is to use the analysis as an initial condition for other mesoscale models, such as the deterministic WRF model. A recent study demonstrated that the 0- to 6-h forecasts with WRF that were initialized with VDRAS analysis significantly improved precipitation forecasts [36]. These techniques are currently being investigated for enhancing wind forecasts.

V. SYSTEM VALUE

The NCAR/Xcel wind power forecasting system is being used for both day-ahead trading and for real-time grid integration. Xcel Energy has performed a thorough cost analysis comparing the impact of the system between 2008 (prior to introduction of the new forecasts), 2009 (the year the wind forecasting system was just beginning to be integrated), and 2010, when the wind power forecasting system was fully integrated [37]–[39].

The day-ahead forecasts feed into the decisions of the energy traders and result in informing generators of the intention to run or not run, commitments of gas units, and setting of incremental prices for the following day [34]. The specifics of the process, and thus, of the cost savings depend on the rules for the particular independent system operating (ISO) market structure. Here we focus on the outcome for one service area, PSCo as seen in Fig. 14, which plots the mean absolute percentage error (MAPE), normalized by system capacity. Note that PSCo is a region in complex terrain, an environment which has been shown to be difficult to forecast [2]. The baseline for comparison is the forecast used by Xcel Energy before implementing NCAR's system. In 2008 and most of 2009, Xcel meteorologists downloaded winds from the North American Mesoscale Model
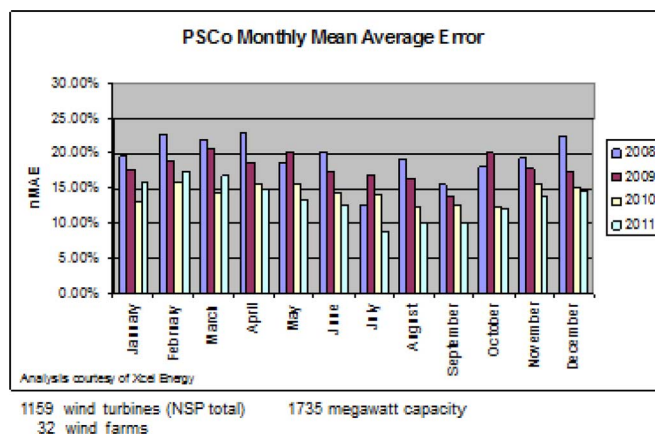
(NAM) and used data soundings from nearby major wind centers as proxies for a wind plant's wind speed forecast. The wind speeds forecast between 45 and 80 m above ground level were used as a proxy for hub height wind speed. Power conversion was accomplished with the manufacturer's power curve, then scaled by the number of turbines at the wind plant and further adjusted for wind plant turbine availability. Initial operating capability of the NCAR system came online in November 2009 and improvements were made periodically through 2011. A decrease in MAPE between 2009 and 2010 occurred every month with a total reduction from 18% in 2009 (before the system was operational) to 14.3% in 2010 for a total decrease of 20% in MAPE. In 2011, there was a slight increase in MAPE as compared to 2010 for the first three months (while remaining below the 2009 level). This increase is directly traceable to several severe icing events (the system does not currently forecast icing). Then the MAPE continued to decrease for the rest of 2011. Similar decreases in error were observed for NSP and somewhat lower decreases for SPS, which has different governing rules and was the last system to implement the forecast system.

Xcel has analyzed the annualized savings for improved forecasting from one year to the next using rigorous industry cost estimation methods. Between 2009 and 2010, they estimate a savings across the three systems of approximately $6.0 M [38]. The improvements continued throughout 2011 and they estimate an additional $2.0 M savings on top of the 2010 figure. These savings are due to more efficient commitment and dispatching of fossil fuel resources.

It is more difficult to break out the impact of wind power forecasting on real-time operations. At this point, however, Xcel grid operators are comfortable with decommitting large coal units when sustained wind events are predicted.

Another useful metric is assessing at what point a wind power prediction system becomes more accurate than a persistence forecast. By mid-2010, the NCAR system performed better than persistence at one hour lead times as seen in Fig. 15.

VI. SUMMARY AND CONCLUSION

The NCAR/Xcel Energy integrated wind power forecasting system components have been described in this paper. The phi-
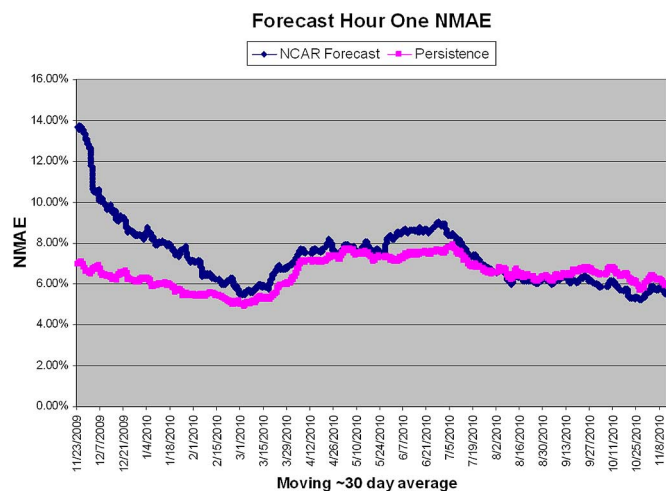
Fig. 15.   Evolution of the 30-day running average NMAE of the DICast prediction at one hour lead time.

losophy espoused here emphasizes blending of multiple technologies in a way that takes advantage of their respective prediction skill across the forecast time horizon. The system was designed to take advantage of real-time wind, power, and availability data from the wind farms and turbines, predicting wind at each turbine, and using empirical power curves to translate from wind speed to power output.

To that end, the system is configured to include tailored high resolution mesoscale model data with assimilation (RTFDDA) of wind farm-specific data, including the nacelle winds; a 30-member mesoscale ensemble system (E-RTFDDA); model data from the national centers; ANalog-space Kalman Filter (ANKF) and a quantile regression (QR) calibration scheme; a statistical forecasting system (DICast) to perform MOS and optimize weights to best match the nacelle wind speeds; empirical power conversion; and a nowcasting system based on VDRAS. Note that other system components are currently being tested, including an observation-based expert system for short-term forecasting and several data mining applications (to determine availability and to assess icing, high speed cutouts, and cold temperature cutouts). This wind power forecasting system began accruing financial benefits to Xcel Energy shortly after it was implemented and saved Xcel Energy approximately $6.0 M in 2010 alone.

There are still many issues to be addressed in wind power forecasting. Forecasting wind power ramps is in its infancy and many advances remain to be made. Physical modeling of icing conditions has not yet been adequately demonstrated. Forecasting wind power for offshore wind farms has just begun in Europe and has not been adequately addressed in the U.S. A plethora of other enhancements and other approaches to the forecasting problem are forthcoming. But this and other work has certainly demonstrated the value of wind power forecasting and how having such a system can enable grid integration of this variable resource by both enhancing system reliability and improving the economics of wind power.

REFERENCES

[1] U.S. Department of Energy, Energy Efficiency and Renewable Energy, 20% Wind Energy by 2020 DOE/GO-102008-2567, Jul. 2008 [Online]. Available: http://www.20percentwind.org/

[2] G. Giebel and G. Kariniotakis, in *Best Practice in Short-Term Forecasting—A Users Guide. European Wind Energy Conference and Exhibition*, Milan, IT, May 7–10, 2007 [Online]. Available: http://powwow.risoe.dk/publ.htm

[3] C. Monteiro, R. Bessa, V. Miranda, A. Botterud, J. Wang, and G. Conzelmann, Wind Power Forecasting: State-of-the-Art 2009 Argonne National Laboratory, Argonne, IL, ANL/DIS-10-1, Nov. 2009.

[4] W. C. Skamarock and J. B. Klemp, "A time-split nonhydrostatic atmospheric model for research and NWP applications," *Special Issue on Environmental Modeling, J. Comp. Phys.*, pp. 3465–3485, 2007.

[5] R. A. Anthes and T. T. Warner, "Development of hydrodynamic models suitable for air pollution and other mesometeorological studies," *Mon. Weather Rev.*, vol. 106, pp. 1045–1078, 1978.

[6] J. E. Hoke and R. A. Anthes, "The initialization of numerical models by a dynamic initialization technique," *Mon. Weather Rev.*, vol. 104, pp. 1551–1556, 1976.

[7] D. R. Stauffer and N. L. Seaman, "Use of four-dimensional data assimilation in a limited-area mesoscale model. Part I: Experiments with synoptic-scale data," *Mon. Weather Rev.*, vol. 181, pp. 1250–1277, 1990.

[8] D. R. Stauffer and N. L. Seaman, "Multiscale four-dimensional data assimilation," *J. Appl. Meteor.*, vol. 33, pp. 416–434, 1994.

[9] Y. Liu, T. T. Warner, J. F. Bowers, L. P. Carson, F. Chen, C. A. Clough, C. A. Davis, C. H. Egeland, S. Halvorson, T. W. Huck, Jr., L. Lachapelle, R. E. Malone, D. L. Rife, R.-S. Sheu, S. P. Swerdlin, and D. S. Weingarten, "The operational mesogamma-scale analysis and forecast system of the U.S. Army Test and Evaluation Command. Part 1: Overview of the modeling system, the forecast products," *J. Appl. Meteor. Clim.*, vol. 47, pp. 1077–1092, 2008a.

[10] Y. Liu, T. T. Warner, E. G. Astling, J. F. Bowers, C. A. Davis, S. F. Halvorson, D. L. Rife, R.-S. Sheu, S. P. Swerdlin, and M. Xu, "The operational mesogamma-scale analysis and forecast system of the U.S. Army Test and Evaluation Command. Part 2: Inter-range comparison of the accuracy of model analyses and forecasts," *J. Appl. Meteor. Clim.*, vol. 47, pp. 1093–1104, 2008b.

[11] Y. Liu, F. Chen, T. Warner, and J. Basara, "Verification of a mesoscale data assimilation and forecasting system for the Oklahoma City area during the Joint Urban 2003 Field Project," *J. Appl. Meteor. Clim.*, vol. 45, pp. 912–929, 2006.

[12] Y. Liu, T. Warner, Y. Liu, C. Vincent, W. Wu, B. Mahoney, S. Swerdlin, K. Parks, and J. Boehnert, "Simultaneous nested modeling from the synoptic scale to the LES scale for wind energy applications," *J. Wind Eng. Ind. Aerodyn.*, 2011, DOI: 10.1016/j.jweia.2011.01.013.

[13] Y. Liu, M. Xu, J. Hacker, T. Warner, and S. Swerdlin, "A WRF and MM5-based 4-D mesoscale ensemble data analysis and prediction system (E-RTFDDA) developed for ATEC operational applications," in *Proc. 18th Conf. Numerical Weather Prediction*, Park City, UT, Jun. 25–29, 2007, AMS.

[14] L. Delle Monache, T. Nipen, X. Deng, Y. Zhou, and R. B. Stull, "Ozone ensemble forecasts: 2. A Kalman filter predictor bias-correction," *J. Geophys. Res.*, vol. 111, p. D05308, 2006, DOI: 10.1029/2005JD006311.

[15] L. Delle Monache, J. Wilczak, S. McKeen, G. Grell, M. Pagowski, S. Peckham, R. B. Stull, J. McHenry, and J. McQueen, "A Kalman-filter bias correction of ozone deterministic, ensemble-averaged, and probabilistic forecasts," *Tellus B*, vol. 60, pp. 238–249, 2008.

[16] L. Delle Monache, T. Nipen, Y. Liu, G. Roux, and R. Stull, "Kalman filter and analog schemes to post-process numerical weather predictions," *Mon. Weather Rev.*, 2011, in press.

[17] T. Hopson, J. Hacker, Y. Liu, G. Roux, W. Wu, J. Knievel, T. Warner, S. Swerdlin, J. Pace, and S. Halvorson, "Quantile regression as a means of calibrating and verifying a mesoscale NWP ensemble," in *Prob. Fcst Symp.*, Atlanta, GA, Jan. 17–23, 2010, American Meteorological Society.

[18] W. Myers, G. Wiener, S. Linden, and S. E. Haupt, "A consensus forecasting approach for improved turbine hub height wind speed predictions," in *Proc. WindPower 2011*, Anaheim, CA, May 24, 2011.

[19] H. R. Glahn and D. A. Lowry, "The use of model output statistics (MOS) in objective weather forecasting," *J. Appl. Meteor.*, vol. 11, pp. 1203–1211, 1972.

[20] G. Young, "Combining forecasts for superior prediction," in *Proc. 16th Conf. Probability and Statistics Atmospheric Science*, Orlando, FL, Jan. 13–17, 2002, pp. 107–111.

[21] S. Gerding and B. Myers, "Adaptive data fusion of meteorological forecast modules," in *Proc. 3rd Conf. Artificial Intelligence Applications, 83rd Amer. Meteor. Soc., Annual Meeting*, Long Beach, CA, Feb. 9–13, 2003.

[22] S. Greybush, S. Haupt, and G. Young, "The regime dependence of optimally weighted ensemble model consensus forecasts of surface temperature," *Weather Forecast.*, vol. 23, no. 6, pp. 1146–1161, Dec. 2008, DOI: 10.1175/2008WAF2007078.1.

[23] W. Myers and S. Linden, "A turbine hub height wind speed consensus forecasting system," in *Proc. AMS Ninth Conf. Artificial Intelligence and its Applications to the Environmental Sciences*, Seattle, WA, Jan. 23–27, 2011.

[24] F. A. Eckel and C. F. Mass, "Aspects of effective mesoscale, short-range forecasting," *Weather Forecast.*, vol. 20, pp. 328–350, 2005.

[25] E. Ela and J. Kemper, Wind Plant Ramping Behavior National Renewable Energy Laboratory, Tech. Rep. NREL/TP-550-46938, 2009.

[26] H. Zheng and A. Kusiak, "Prediction of wind farm power ramp rates: A data-mining approach," *J. Solar Energy Eng.*, vol. 131, pp. 031011-1–031011-8, 2009.

[27] J. Sun and N. A. Crook, "Dynamical and microphysical retrieval from Doppler radar observations using a cloud model and its adjoint: Part I. model development and simulated data experiments," *J. Atmos. Sci.*, vol. 54, pp. 1642–1661, 1997.

[28] B. Wu, J. Verlinde, and J. Sun, "Dynamical and microphysical retrievals from Doppler radar observations of a deep convective cloud," *J. Atmos. Sci.*, vol. 57, pp. 262–283, 2000.

[29] J. Sun and N. A. Crook, "Real-time low-level wind and temperature analysis using single WSR-88D data," *Weather Forecast.*, vol. 16, pp. 117–132, 2001.

[30] A. Crook and J. Sun, "Assimilating radar, surface and profiler data for the Sydney 2000 forecast demonstration project," *J. Atmos. Oceanic Technol.*, vol. 19, pp. 888–898, 2002.

[31] J. Sun, M. Chen, and Y. Wang, "A frequent-updating analysis system based on radar, surface, and mesoscale model data for the Beijing 2008 forecast demonstration project," *Weather Forecast.*, vol. 25, pp. 1715–1735, 2010.

[32] E. Kessler, "On the distribution and continuity of water substance in atmospheric circulations," *Meteor. Monogr.*, vol. 32, Amer. Meteor. Soc., 1969, 84 pp..

[33] J. Sun and Y. Zhang, "Assimilation of multiple WSR_88D Radar observations and prediction of a squall line observed during IHOP," *Mon. Weather Rev.*, vol. 136, pp. 2364–2388, 2008.

[34] J. Sun, Y. Zhang, G. Wiener, N. Oien, and W. Mahoney, "A rapid-updated wind analysis system based on mesoscale model, radar, and surface data for ramp-event wind energy forecasting," in *Proc. AMS Second Conf. Weather, Climate and the New Energy Economy*, Seattle, WA, Jan. 23–27, 2011.

[35] A. Caya, A. Crook, and J. Sun, "The use of an evaporation scheme in a boundary-layer model for real-time 4D-Var radar data assimilation and forecasting of convergence lines," in *Preprint: 31st Conference on Radar Meteorology*, Seattle, WA, 2003, pp. 110–113, Amer. Meteor. Soc..

[36] Y.-C. Liou, S.-L. Tai, J. Sun, and S.-F. Zhang, "Quantitative precipitation forecast using Doppler radar data, a cloud model equipped with adjoint, and WRF model—An application to a case study during 2008 SoWMEX in Taiwan," *Weather Forecast.*, 2011, submitted for publication.

[37] K. Parks, Y.-H. Wan, G. Wiener, and Y. Liu, Wind Energy Forecasting—A Collaboration of the National Center for Atmospheric Research (NCAR) and Xcel Energy National Renewable Energy Laboratory, Golden, CO, Jun. 2011.

[38] K. Parks, "Xcel energy/NCAR wind energy forecasting system," in *Proc. Utility Wind Integration Group Variable Generation Forecasting Applications to Utility Planning and Operations Meeting*, Albany, NY, Feb. 23–24, 2011.

[39] K. Parks, "Wind energy integration and forecasting: What is it worth?," in *Proc. Int. Conf. Energy and Meteorology*, Gold Coast, Australia, Nov. 8–11, 2011.

William P. Mahoney received the B.S. degree in aeronautics from Miami University of Ohio in 1981, and the M.S. degree in atmospheric science from the University of Wyoming in 1983.

He is the Deputy Director of the Research Applications Laboratory (RAL) at the National Center for Atmospheric Research (NCAR). He has been involved in research and development activities at NCAR for more than 25 years and has directed programs in aviation, surface transportation, social sciences, agriculture, intelligent forecast systems, and renewable energy. He has written or coauthored more than 40 papers and frequently presents NCAR's work at national and international conferences and seminars.

Mr. Mahoney is a fellow of the American Meteorological Society (AMS).

Keith Parks received the B.E. degree from the University of Auckland in New Zealand.

He is currently Director of Business Development (Energy) at Global Weather Corporation. Previously, he was a Senior Analyst with Xcel Energy Services, Inc. Xcel Energy is the largest provider of wind energy and fifth largest combined electricity and natural gas utility in the United States. He manages grid integration of over 4.2 GW of installed wind energy across seven states (Texas, New Mexico, Colorado, North Dakota, South Dakota, Minnesota, and Wisconsin). He is an expert in renewable integration cost calculation and mitigation strategies. Previously, he held positions with the National Renewable Energy Laboratory (NREL) and energy consulting firms specializing in electricity energy modeling, resource planning, and grid operations.

Gerry Wiener was born in Los Angeles, CA on January 30, 1952. He graduated *summa cum laude* in mathematics from U.C. Berkeley in 1971 and received the doctorate degree in mathematics from the University of Colorado in 1980.

He has been employed at the National Center for Atmospheric Research since 1987 where he has worked on microburst and wind shear detection systems, turbulence detection and forecasting systems, and wind/power forecasting systems. His special interests are in data mining, statistical postprocessing, and systems engineering. Wiener received the NCAR Scientific and Technical Advancement Award in 1988 for joint work in developing a display system for the terminal Doppler weather radar.

Yubao Liu received the Graduate Diploma in computer science and the Ph.D. degree in atmospheric science.

He is a project scientist with the National Center for Atmospheric Research. He has 24 years of experience in mesoscale and small-scale weather modeling. He published 30 papers in referred weather journals and presented his research at numerous national and international conferences. His special research interests are in meso- and small-scale data assimilation, ensemble forecasting, and atmospheric physics processes and their parameterization. He has been a lead modeler of the NCAR real-time four-dimensional data assimilation and forecasting system and its extension of ensemble capability.

William L. Myers received the B.A. degree in mathematics and French from Dartmouth College in 1980, the M.A. degree in mathematics from the University of Washington in 1982, and the Ph.D. degree in computer science from the University of Colorado in 2001.

He is a Software Engineer at the Research Applications Laboratory (RAL) at the National Center for Atmospheric Research (NCAR). He has been involved in applied atmospheric research and the development of decision support systems at NCAR since 1987. His interests are machine learning, statistical postprocessing, computer graphics, and user interface design. He has been a primary developer of the (Dynamic Integrated ForeCast) DICast system. He has served on the Committee on Artificial Intelligence Applications of the American Meteorological Society (AMS).

Thomas Hopson received the B.A. degree in physics from Rice University in 1989, the M.S. degree in civil engineering from the University of Colorado in 1997, and the Ph.D. degree in astrophysical, planetary, and atmospheric sciences from the University of Colorado in 2005.

He is a scientist with the National Center for Atmospheric Research (NCAR). Before joining NCAR, he worked on river geomorphology for the U.S. Geological Survey, and was a Fulbright Scholar to Zimbabwe. He works on ensemble weather, disease, and flood forecasting applications, including ensemble verification and pre- and postprocessing issues, and serves on the Hydrologic Ensemble Prediction Experiment (HEPEX) committee. He has coauthored a book chapter, and numerous journal articles, conference papers, and technical reports.

Juanzhen Sun received the B.S. degree from Lanzhou University of China and the M.S. and Ph.D. degrees from the University of Oklahoma.

She has been a scientist at the National Center for Atmospheric Research (NCAR) for the past 19 years. Her main research interests are mesoscale and convective-scale data assimilation, high-impact weather study, and short-term numerical weather prediction. She is recognized as a leader in the area of radar data assimilation for nowcasting applications. She received the outstanding publication award from NCAR in 2001 for three of her publications that led the research on the use of radar observations for numerical weather prediction.

David Johnson received the B.A. degree in physics from Ripon College in 1967, and the Ph.D. degree in geophysical sciences from the University of Chicago in 1979.

He is a Project Scientist with the Research Applications Laboratory at the National Center for Atmospheric Research (NCAR). He has been at NCAR for over 20 years, working in a variety of areas of remote sensing and physical meteorology. In addition to his recent work in the wind energy field, he has also been active in developing applications to enhance aviation safety, making use of both satellite and ground-based observations.

Dr. Johnson was a 2007 recipient of the NASA Paul Halloway Technology Transfer Award.

Luca Delle Monache received the Laurea (M.S.) degree in mathematics from the University of Rome, Italy, in 1997, the M.S. degree in meteorology from the San Jose State University, San Jose, CA, in 2002, and the Ph.D. degree in atmospheric sciences from the University of British Columbia, Vancouver, Canada, in 2006.

He is a scientist with the National Center for Atmospheric Research (NCAR). Before joining NCAR he worked at the Lawrence Livermore National Laboratory. His main interests include mesoscale numerical weather prediction, ensemble data assimilation, boundary layer, air pollution, urban meteorology, and dispersion modeling. He currently serves on the AMS ad-hoc Committee on Generating and Communicating Forecast Uncertainty, and has authored a book chapter, and over 80 journal articles, conference papers, and technical reports.

Sue Ellen Haupt received the B.S. degree in meteorology from Penn State in 1978, the M.S. degree in engineering management from Western New England College in 1982, the M.S. degree in mechanical engineering from Worcester Polytechnic Institute in 1984, and the Ph.D. degree in atmospheric science from the University of Michigan in 1988.

She is Director of the Weather Systems and Assessment Program at the National Center for Atmospheric Research. She has been on the faculty of The Pennsylvania State University, University of Colorado/Boulder, U.S. Air Force Academy, University of Nevada, Reno, and Utah State University and worked for New England Electric System. She chaired the Committee on Artificial Intelligence Applications of the American Meteorological Society (AMS) and currently chairs the AMS 2012 Wind Power Prediction Contest subcommittee. She has authored over 250 books, book chapters, journal articles, conference papers, and technical reports.